Chaotic scattering off a rotating target

1995 J. Phys. A: Math. Gen. 28 2529

(http://iopscience.iop.org/0305-4470/28/9/014)

J. Phys. A: Math. Gen. 28 (1995) 2529–2544. Printed in the UK

Chaotic scattering off a rotating target

N Meyer†, L Benet†, C Lipp†, D Trautmann†, C Jung‡ and T H Seligman‡
† Institut für Theoretische Physik, Universität Basel, Klingelbergstr. 82, CH-4056 Basel, Switzerland
‡ Instituto de Física, Laboratorio de Cuernavaca, UNAM, Apartado Postal 139-B, 62191 Cuernavaca, Morelos, Mexico

Received 5 October 1994, in final form 16 February 1995

Abstract. We study the classical scattering of a point particle from one and two rotating hard discs in a plane, as an idealization of the scattering off a rotating target. The system displays regular or chaotic behaviour depending on the value of the only constant of motion: the Jacobi integral. We present results on the transition between regular and chaotic behaviour in terms of the periodic orbits of the system. For certain ranges of the Jacobi integral the dynamics is fully hyperbolic. The number of symbols needed to characterize the invariant set is different in each of those intervals and may become arbitrarily high.

1. Introduction

In recent years the interest in the effects of classical chaos in quantum mechanics and its applications in atomic and molecular systems has increased enormously, both for bounded and scattering systems. A lot of work has been done in this direction in connection with Rydberg atoms [1] and the hydrogen atom in a strong magnetic field [2]. The irregular features found in the spectra can be explained in terms of the underlying classical chaotic motion due to the nonlinear potential induced by the strong magnetic field or by the coupling of the hydrogenic orbital motion of the electron and the rotational motion of the nuclei treated as a rigid rotor. In the same way, some advances have been made in connection with scattering systems (see [3] and references therein) where the properties of the fluctuating part of the S-matrix are related with the classical behaviour of the system.

For twenty years in physical chemistry classical models for reactive scattering have been investigated using full three-body interaction potentials. For a review see [4]. The complication here is related to the large number of degrees of freedom for the general problem, apart from the complications that might arise from the nonlinear dynamics. In this direction, Wintgen and co-workers have studied the case of the helium atom in two dimensions [5] and recently found a new class of periodic orbits whose existence is a true three-body effect. The less studied case of scattering systems has been mainly approached in astronomy in connection with the satellite-capture problem, but those studies have been focused to the fractal structure displayed on the initial-value space as a function of an outgoing condition [6].

The aim of the present paper is to shed some light on the problem of rotating targets. As a simple model for a rotating target we take either one or two hard discs moving along a circle with constant speed.

The model with two discs may be viewed as a model for two relevant physical processes. On one hand it relates to the astronomical reduced three-body problem (RTBP) with repulsive

0305-4470/95/092529+16$19.50

forces. On the other hand it is relevant to the scattering of an electron off a rotating diatomic molecule. Note that in both cases energy transfer to the rotating core is excluded.

The model with one disc is used as the simplest version of a rotating target since it already shows the qualitative features which turn out to be important in the two-disc model. A discussion of the differences will show that a salient feature of the two-disc model is the existence of a periodic orbit for arbitrarily high energies, which is absent with a single disc.

The system is introduced in section 2 where the only integral of motion is derived, namely the Jacobi integral. In section 3 we study numerically the initial value space and some quantities that characterize the outgoing states. There, we find parameter ranges where chaotic scattering occurs. In section 4, the periodic orbits are fully characterized in terms of some primitive periodic orbits that are the skeleton of the dynamics of the system. These primitive periodic orbits are obtained analytically, and the homoclinic connections between such orbits determines whether regular or irregular scattering occurs. The invariant manifolds of the primitive periodic orbits are used in section 5 to discuss the transition between different kinds of dynamics that arise in this system. Information about the stability of such orbits is obtained. Section 6 is devoted to the discussion of the two-disc system, i.e. the reduced three-body system. A summary of our results and conclusions are presented in section 7.

2. The rotating disc model and the Jacobi integral

The RTBP is defined [7, 8] as the motion of a light point particle in a plane under the action of gravitational forces due to two massive bodies. The massive bodies revolve around their centre of gravity under their mutual attraction in (closed) Kepler orbits, independently of the presence of the projectile. From here on, we will refer to the system formed by the massive bodies as the binary. In the limit of infinite mass for the binary the Hamiltonian of this system may be expressed as the motion of a single particle in a time-dependent potential. Taking the centre of gravity as the origin of Cartesian X–Y coordinates, the Hamiltonian of the system is given by

$$H = \tfrac{1}{2}(P_x^2 + P_y^2) + V(X, Y, t) \tag{1}$$

where the potential $V(X, Y, t)$ depends explicitly on time through the terms involving the positions of the primaries, $R_i(t)$ for $i = 1, 2$. Then, the energy of the system is no longer a constant of motion.

We will investigate only the case where the motion of the binary is circular, and for simplicity we consider models where the primaries have equal mass, although this is not necessary for the following. Because of the particular symmetry of the circle, we can reduce the dynamics of the system by passing to a rotating reference frame. Instead of writing the Hamiltonian in a static (sidereal) coordinate system, we use a frame of reference (synodic) that rotates with the same angular velocity as the primaries do. We choose the new x-axis as the line joining the primaries. Then, by means of a canonical transformation (indeed a point contact transformation) with the generating function given by

$$W = P_x(x\cos\omega t - y\sin\omega t) + P_y(x\sin\omega t + y\cos\omega t) \tag{2}$$

we obtain the new Hamiltonian

$$J = \tfrac{1}{2}(p_x^2 + p_y^2) + V(x, y) - \omega(xp_y - yp_x)\,. \tag{3}$$

This new Hamiltonian J does not involve time explicitly, so it corresponds to an integral of motion, the so-called *Jacobi integral*. The Jacobi integral can be written in terms of the old coordinates in the sidereal frame, having exactly the same analytical expression as (3).

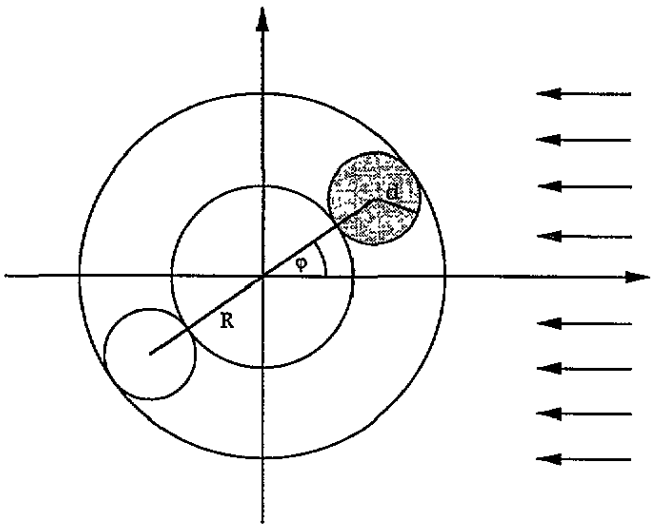

Figure 1. Geometry of the two-disc system. The hard discs of radius d rotate with constant angular velocity ω on a circular orbit. The distance between the centres is $2R$. The initial phase of the discs, i.e. the angular position when the particle enters the interaction region is φ.

It should also be mentioned that the existence of the Jacobi integral depends strongly on the particular symmetry of the circular orbit of the binary, and does not exist when the motion is elliptic. This results from the constant angular velocity of the binary for circular motion. After performing the same canonical transformation as before, for the elliptic case the primaries still vibrate anharmonically giving rise to the explicit appearance of time in the new Hamiltonian.

First we consider the classical motion of a free particle in a plane scattered by one massive disc of radius d that rotates on a circular orbit of radius $R > d$ with constant angular velocity ω and whose motion is not affected by the collision with the particle (figure 1). As we shall see below, this system and the two-disc system display the same qualitative features. In both cases, the Hamiltonian is given by (1) and the Jacobi integral (3) remains a constant of motion. The potential appearing in (1) and (3) is zero everywhere except inside the discs, where it has an infinite value.

The dynamics in the sidereal coordinate system for the model are straightforward since the velocity between bounces remains constant. Note that the particle is accelerated when it collides with the front of a disc (with respect to the rotation), decelerated when it collides with the back, and keeps the same velocity when it collides radially (figure 2). We decompose the velocity vectors of the projectile and the collision point on the disc into a parallel and a perpendicular component relative to the tangent of the disc at the collision point. Then the outgoing velocities (in the sidereal coordinate system) are given by

$$v_{\parallel}^{(\mathrm{out})} = v_{\parallel}^{(\mathrm{in})} \tag{4}$$

$$v_{\perp}^{(\mathrm{out})} = 2V_{\perp} - v_{\perp}^{(\mathrm{in})} \tag{5}$$

where $V_{\perp}$ is the perpendicular velocity of the collision point.

In both limiting cases $\omega = 0, \infty$ the target consists of one static disc of radius d or $R + d$, respectively. The system is integrable as energy and angular momentum are two independent constants of the motion. No localized orbits are accessible to the scattering

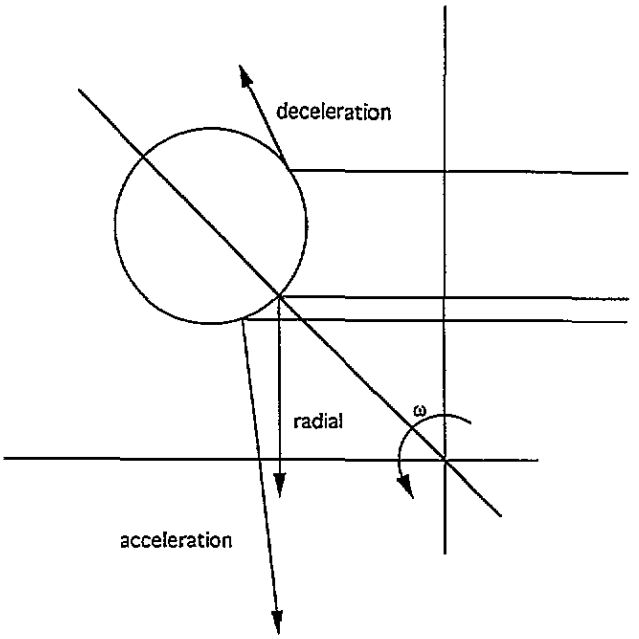

Figure 2. Effects on the velocity of the projectile after a collision with a moving disc: the particle is accelerated if it collides on the front of the disc (with respect to the rotation), decelerated on the rear and keeps the energy constant if it bounces radially.

motion. In contrast, in the two-disc system for $\omega = 0$ the scattering trajectories can approach the periodic orbit that lies on the line joining the centres of the discs.

3. Chaotic and regular scattering: numerical results

In this section we present results for the model introduced in the preceding section. We choose the radius of the disc $d = 1$, the radius of the circular orbit $R = 3$, and the angular velocity of the disc $\omega = 1.0$. The sense of rotation of the disc is counterclockwise. We choose the initial velocity of the projectile as negative and parallel to the x-axis. The impact parameter is given by the initial value of the Y coordinate. The origin is the centre of the circular orbit. The impact parameter, the initial velocity and the initial phase of the disc define the initial conditions for the system. The disc starts to revolve when the particle enters the interaction region $(x^2 + y^2 < (R + d)^2)$.

There are two kinds of scattering experiments that we have studied so far. On the one hand, we considered for every impact parameter the same initial velocity (or initial energy). This means that two different impact parameters correspond to different Jacobi integrals. On the other hand, we fixed the Jacobi integral throughout the impact parameter range. In both cases, we performed Monte Carlo calculations on the initial conditions space (initial phase $\varphi \in [0, 2\pi)$ and impact parameter $b = y_0 \in [-R-d, R+d]$) and studied the structure of this (b, φ)-plane for 0, 1, 2, 3, ... bounces. For fixed initial phase, we studied the time delay, the length increment of the trajectories, the number of bounces and the scattering angle to characterize the outgoing state. The time delay and length increment of the path in the interaction region are referred to those of the free particle, i.e. a particle which does not bounce with the disc has time delay and length increment equal to zero.

3.1. Constant initial energy

In figure 3 we show a Monte Carlo calculation in the initial conditions space (b, φ) when we shoot with constant initial velocity $v_x^{\text{init}} = -1.0$. Each frame in this figure represents those initial conditions whose number of bounces is equal to 0, 1, 2, and 3 or more, respectively. The region where a large number of bounces is found lies approximately between 0 and 2 for the impact parameter and 3 and 3.5 for the initial phase (modulo 2π). The (self-similar) snail-structures are responsible for the chaotic behaviour in the system. In figure 4(a) we plot the time delay and the number of bounces as a function of the impact parameter for constant initial phase $\varphi = 3.33$ and $v_x^{\text{init}} = -1.0$; figures 4(b) and (c) show successive enlargements of figure 4(a). The self-similar and fractal structure of the subset of impact parameters that lead to wild fluctuations and singularities on the functions is clearly visible. Topological chaos is then found in the system [3, 9]. Beside the self-similarity, in figures 4(b) and (c) we also note that the distance between neighbouring peaks from the infinite sequence of singularities becomes smaller in a geometrical progression displaying accumulation points. Here, very long time delays are reached without increasing significantly the number of bounces. The corresponding orbits loose after a few bounces almost all the energy, so the time needed for the next bounce rises up considerably. These orbits are the analog to the parabolic orbits that reach infinity with velocity equal zero in the Kepler problem.

Since the system is invariant to scale transformations (just as billiards do), the dynamics are preserved when the ratio $\rho = v_x^{\text{init}}/\omega$ is constant. Chaotic scattering is found for $\rho \approx 1$. For v_x^{init} small compared to ω, the projectile is scattered out of the interaction region mainly

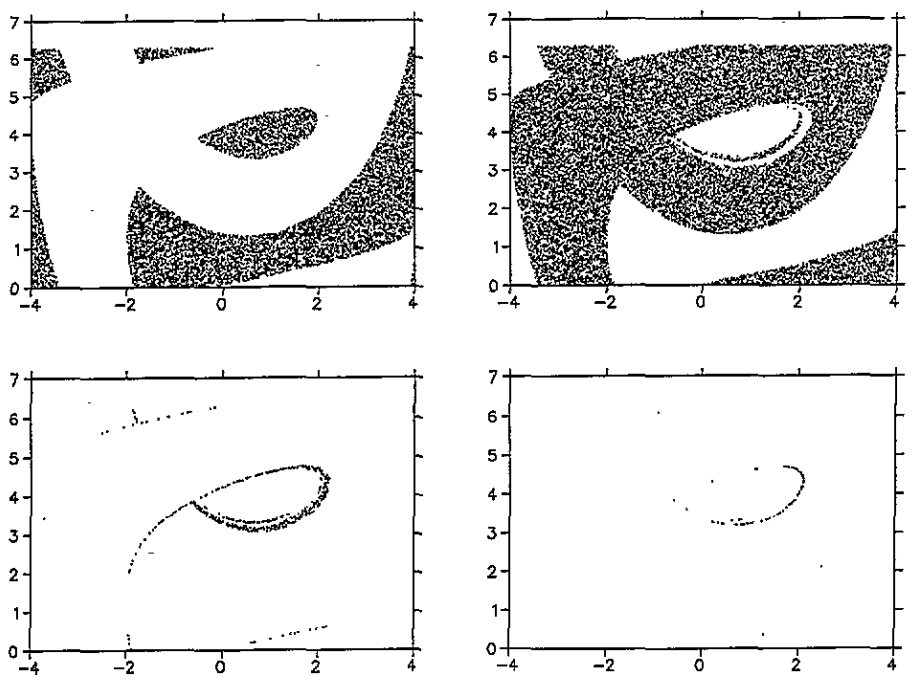

Figure 3. Calculation with Monte Carlo choice for the initial conditions in the one-disc model. We mark the initial conditions leading to escape after (a) zero, (b) one, (c) two and (d) three or more bounces. All initial conditions have the same initial energy for the projectile ($v_x^{\text{init}} = -1.0$, $\omega = 1.0$).

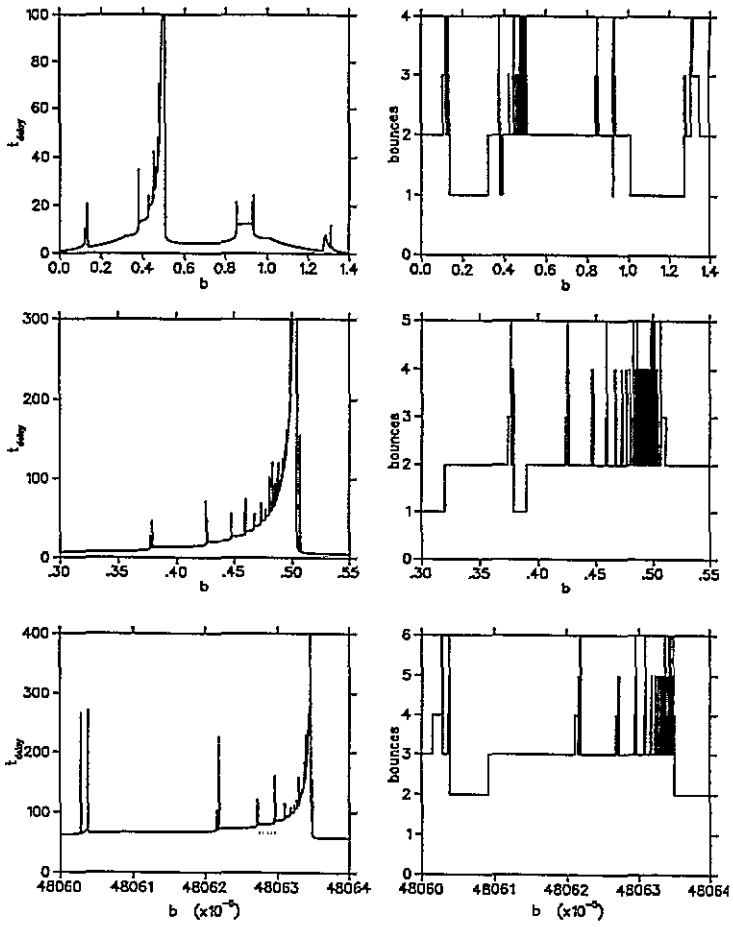

Figure 4. (*a*) Time delay and number of bounces as function of the impact parameter for a fixed initial phase of the discs $\varphi_{\text{init}} = 3.33$ when shooting with constant initial energy ($v_x^{\text{init}} = -1.0$, $\omega = 0.75$) in the one-disc model. (*b*), (*c*) Enlargements of a region of (*a*) showing the self-similar geometry.

in the first bounce, so the snail-structures as in figure 3 are erased. In the opposite case, although a larger number of bounces might be found, the regions in the initial condition space have no fractal structure.

3.2. Constant initial Jacobi integral

For the experiments with constant initial energy, although the Jacobi integral was conserved for every single trajectory, we were comparing the behaviour of initial conditions with different constants of motion. This means that we were studying the complete phase space of the problem. By fixing the Jacobi integral for every impact parameter we reduce the study of the dynamics to a subshell of the phase space. As we will see in the following sections, it is possible to explain the behaviour shown for the constant initial energy experiments in terms of the different characteristics of the Jacobi integral subshells.

In figures 5 we show Monte Carlo results for the number of bounces in the initial conditions space for $J = 1.0$. The same kind of snail-structures as in figures 3 are found

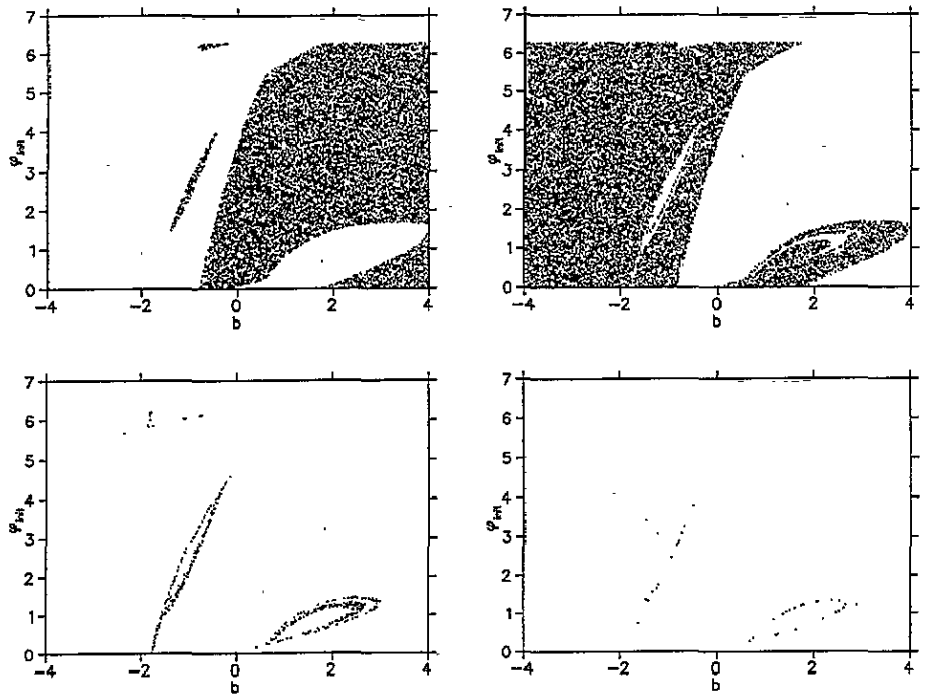

Figure 5. Calculation with Monte Carlo choice for the initial conditions in the one-disc model. We mark the initial conditions leading to escape after (*a*) zero , (*b*) one, (*c*) two and (*d*) three or more bounces. All initial conditions have the same Jacobi integral ($J = 1.0$, $\omega = 1.0$).

again. Figures 6(*a*)–(*c*) show the fractal structures for the time delay and the number of bounces for a constant initial phase $\varphi = 1.2$. In contrast to figures 4(*a*)–(*c*), where a (self-similar) accumulation of singularities was found, figures 6(*a*)–(*c*) do not display any accumulation effect. In this case the plots of time delay and number of bounces are equivalent. As we will see below, the case $J = 1.0$ is completely hyperbolic, so there are no remnants of marginal stability (neither KAM-tori nor stable periodic orbits). In the case of constant initial energy, since the initial conditions correspond to different Jacobi integrals, the complete hyperbolicity within certain manifolds of constant J might not be apparent. Indeed, the accumulation points shown in figure 4(*b*) and (*c*) correspond to small values of the Jacobi integral where regions of stability were found.

The chaotic snail-structures as shown in figures 5 conserve the scaling properties as before. For larger Jacobi integral the particle has larger incoming velocity so the snail shrinks after a few bounces until it disappears, leading then to regular scattering (although the system is not completely integrable). When reducing the Jacobi integral we still find complicate structures like those shown, all maintaining the fractal properties. Indeed, even for negative Jacobi integrals the same self-similar behaviour is found up to a minimal value. Lowering furthermore the value of the Jacobi integral re-establishes the regular behaviour in the system. This global behaviour in terms of the Jacobi integral will be explained in the following sections.

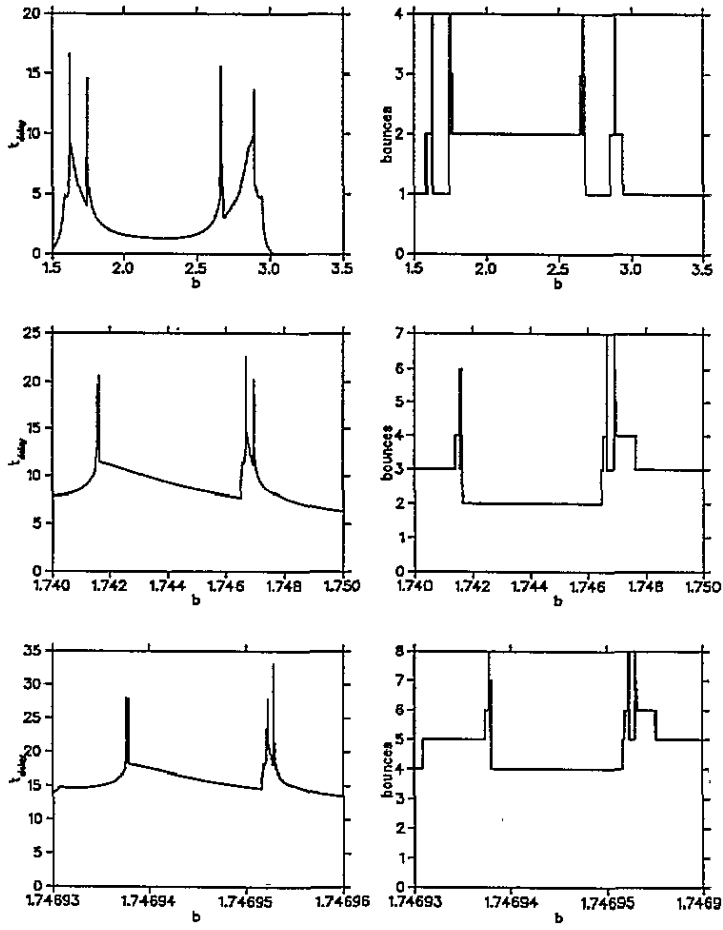

Figure 6. (*a*) Time delay and number of bounces as function of the impact parameter for a fixed initial phase of the disc $\varphi_{\text{init}} = 1.2$ when shooting with $J = 1.0$, $\omega = 1.0$. (*b*), (*c*) Enlargements of a region of (*a*) showing the self-similar geometry.

4. Periodic orbits

In this section our goal is to understand the periodic orbit structure and relate it to the singularities in the deflection function described in the preceding section. If the incoming particle bounces radially its energy remains constant and the incoming and outgoing angles coincide. The simple periodic orbits keep the angles between bounces constant and are inscribed in the inner circle defined by the motion of the disc. These primitive periodic orbits have the same geometrical properties as those of the circular billiard. They look like stars or polygons, depending on whether the trajectories do or do not cross (figure 7(*a*)). Indeed, even the orbits with constant energy which are not closed in the sidereal frame (thus being quasi-periodic) are truly periodic in the synodic frame (figure 7(*b*)). As the primitive periodic orbits form the skeleton of the chaotic invariant set it will be essential to study their structure as a function of the Jacobi integral.

Denoting by $\alpha \in [-\pi/2, \pi/2]$ the incoming (outgoing) angle for a radial collision with the convention that α is negative when the projectile runs against the rotation of the disc,

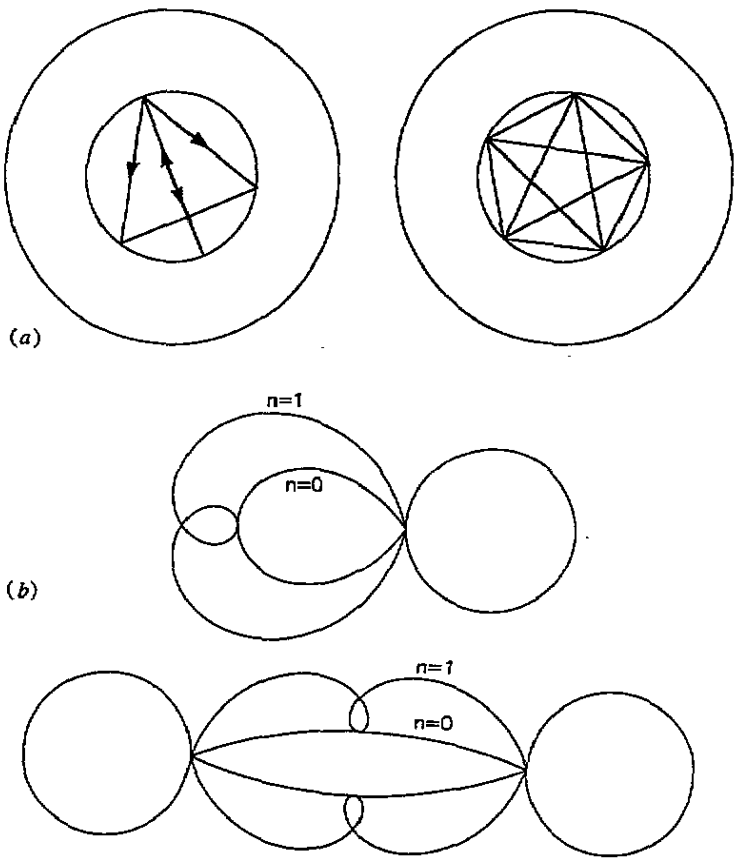

Figure 7. (*a*) Periodic orbits in the sidereal coordinate system. (*b*) Periodic orbits in the synodic coordinate system. The value n denotes the number of complete turns of the discs before the next collision.

the relation between the Jacobi integral and α for these periodic orbits is given by

$$J_{11} = \frac{2\omega^2(R-d)^2}{((2n+1)\pi - 2\alpha)^2}\left[\cos^2\alpha - ((2n+1)\frac{\pi}{2} - \alpha)\sin 2\alpha\right]. \tag{6}$$

Here, n denotes the number of full turns of the disc before the next bounce. The index 11 denotes that the particle is always colliding with the same disc in comparison to the two-disc case. In figure 8 we plot J_{11} as a function of α for $n = 0, 1, 2$. From this figure we can see that for a fixed Jacobi integral we obtain a total of zero, one, two or more intersection points. The number of intersections is precisely the number of primitive periodic orbits allowed for that Jacobi integral, i.e. they are the only periodic orbits on which the energy remains constant. This structure is responsible for the behaviour of the scattering functions described in section 3. If the number of primitive periodic orbits for a fixed Jacobi integral is less than two, the system behaves as a regular scatterer. The system displays chaotic scattering if this number is equal to or greater than two. This implies that for $J > 1.173\,13\ldots$ or $J < -0.457\,71\ldots$ there is no topological chaos.

Figure 8 explains the structure of the scattering functions for constant initial energy experiments (figures 4(*a*) and (*c*)) where the scattering functions displayed accumulation

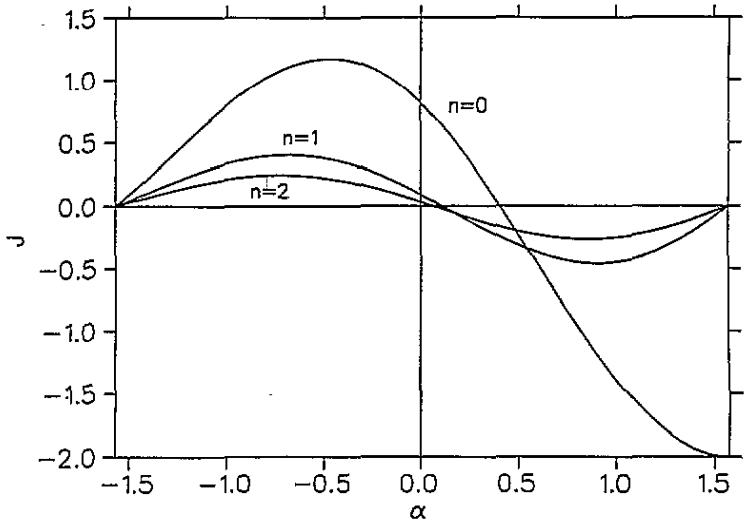

Figure 8. Behaviour of the Jacobi integral for the different primitive periodic orbits as a function of the incidence angle α for radial collisions (equation (6)).

points. There, every impact parameter corresponds to a different value of the Jacobi integral. The accumulation points correspond to small (even slightly negative) J-values where the curves to different n in figure 8 display many intersection points. As will be shown in the next section, when one of the intersection occurs very close to the maximum (or minimum) of one of the curves, stable regions are found. Since the probability that one of the intersections is close to a maximum (or minimum) grows as the absolute value of the Jacobi integral tends to zero i.e. $n \to \infty$, we will then find an increasing number of stable regions.

5. Invariant manifolds of the primitive orbits

In order to understand the details of the curves of figure 8 and the bifurcations to chaotic scattering as a function of the Jacobi integral, we define a Poincaré section in the non-conjugate variables ϕ and α. The angle ϕ corresponds (in the synodic frame) to the angular position where the projectile bounces on the disc. ϕ is measured clockwise from the negative x-axis, i.e. a radial bounce implies $\phi = 0$. α is the angle formed by the outgoing velocity vector in the synodic coordinates referred to the normal line in the collision point, having here the same convention for the signs as introduced in the preceding section in terms of the direction of the rotation of the disc. In terms of these angles, the Jacobi integral is given by

$$J = \tfrac{1}{2}v^2 - \omega v\,[R\sin(\alpha+\phi) - d\sin(\alpha)]\,. \tag{7}$$

Here, $v = (v_\parallel^2 + v_\perp^2)^{1/2}$ denotes the magnitude of velocity after the collision. Since equation (7) is a quadratic equation in v, we have, in principle, two natural ways of defining our Poincaré section in terms of the sign chosen in the square root to define v. For J positive the assignment is straightforward, since one of the roots has no physical meaning and the Poincaré surface of section is uniquely defined. For negative Jacobi integral two different Poincaré sections might be considered since both roots of (7) lead to positive values for the magnitude of the velocity. In the following we consider the Poincaré map defined by the

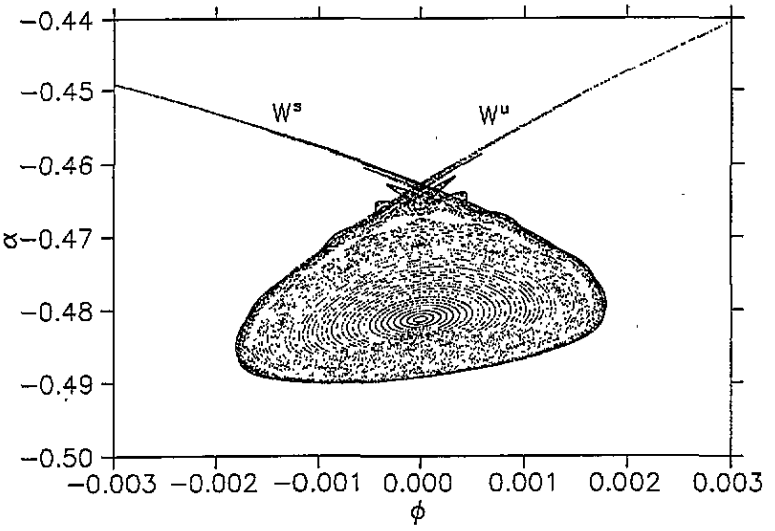

Figure 9. Poincaré plot of the surrounding of the two fixed points for $J = 1.173$. The upper fixed point is hyperbolic and has homoclinic intersections while the lower is elliptic and surrounded by KAM tori.

points in the (ϕ, α)-plane whose magnitude v is greater than $v_{\min} = R\sin(\alpha+\phi) - d\sin\alpha$, i.e. we map just the outgoing conditions that correspond to the positive sign in the square root. Considering this symmetry adapted Poincaré section we ensure that the fixed points (primitive periodic orbits) of our map lie on the line $\phi = 0$.

For Jacobi integrals $J > J_{\max} = 1.173\,13\ldots$, above the maximum of the curve corresponding to $n = 0$ in figure 8, there are no fixed points on the axis $\phi = 0$. Our numerical results showed that indeed there are no fixed points at all. In figure 9 we show the Poincaré section for $J = 1.173$, just below the maximum, where two fixed points are found; one elliptic and the other hyperbolic. This typically occurs after a saddle-centre bifurcation [10]. Topological chaos arises from the homoclinic intersections of the saddle, whereas stable orbits are found around the centre surrounded by KAM-tori and fixed points of higher order. By further decreasing the value of the Jacobi integral the fixed points move apart and the elliptic one becomes inverse hyperbolic by a period-doubling bifurcation ($J \approx 1.170\ldots$). Heteroclinic intersections are immediately found, but the tendrils of the manifolds form an incomplete horseshoe [11]. A complete horseshoe is found at $J \approx 1.160\ldots$. In figure 10 we plot the stable and unstable manifolds for the case $J = 1$, where the fixed points are located at $\alpha_+ \approx -0.146\ldots$ and $\alpha_- \approx -0.817\ldots$ (see figure 8). The heteroclinic intersections form a complete Smale horseshoe. Thus a complete symbolic dynamic with two symbols can be constructed [11]. The fixed point at α_+ is hyperbolic, while the one at α_- is inverse hyperbolic. The eigenvalues of the linearized map increase very fast from the bifurcation at $J \approx 1.173\,13\ldots$ to the case $J = 1$.

Decreasing the Jacobi integral further, a complete binary horseshoe remains until $J \approx 0.41\ldots$. Then some of the tendrils are folded back into the fundamental rectangle leading to new intersections. From here on the invariant set is an incomplete horseshoe with an incomplete symbolic dynamic of four symbols (pruning) [12, 13]. Connected with the homoclinic tangencies are infinite sequences of saddle-centre bifurcations creating further periodic points. The central saddle-centre bifurcation is a creation of two new fixed points.

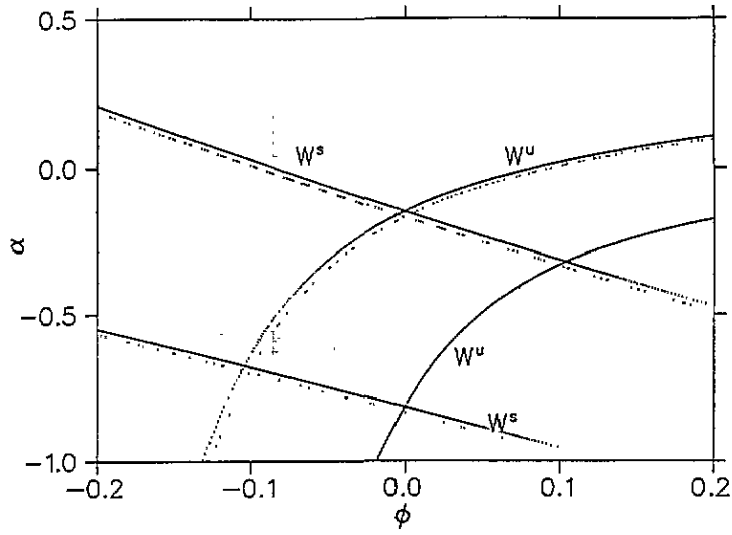

Figure 10. Stable and unstable manifolds for $J = 1.0$. The elliptic fixed point has changed into an inverse hyperbolic one and the dynamics is now completely hyperbolic.

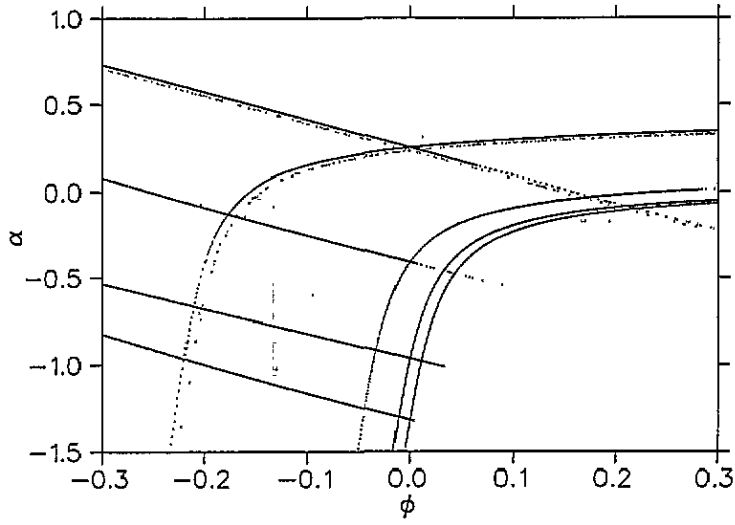

Figure 11. Stable and unstable manifolds for $J = 0.35$. There are four fixed points after a second saddle-centre bifurcation. Again the fully hyperbolic case is reached. Note that the fixed points are located on the line $\varphi = 0$.

This happens exactly at the maximum of the curve $n = 1$ in figure 8. For still lower values of J the invariant sets turns into a complete horseshoe with four symbols. This structure is reached at the value of $J \approx 0.40\ldots$ and remains structurally stable in an interval of J values. In figure 11 we illustrate the stable and unstable manifolds for $J = 0.35$. In this case, there are four fixed points, two hyperbolic and two inverse hyperbolic. This is again a fully hyperbolic case leading to a complete Smale horseshoe. Notice that the new fixed points that appear in the map lie between the points that already existed. The symbolic

dynamic is now built from four symbols, each corresponding to one of the fixed points. Orbits displaying all combinations of these symbols are found numerically.

For lower but still positive values of the Jacobi integral the same scenario as described above takes place for larger n: below the maximum of the n-curve the horseshoe structure is incomplete and is characterized with an incomplete symbolic dynamic of $N = 2n$ symbols. A central saddle-centre bifurcation occurs at the maximum of the n-curve giving rise to the creation of a degenerate fixed point which leads to a hyperbolic and an elliptic fixed point. The elliptic point becomes inverse hyperbolic as the Jacobi integral is further reduced and later a complete horseshoe with $N = 2n$ symbol values develops. Reducing J further, the complete hyperbolicity is lost and a new incomplete horseshoe is found which can be then described with an incomplete symbolic dynamic of $N' = 2(n+1)$ symbols etc.

In the case of a negative Jacobi integral, the scenario is inverted in the sense that the extrema found for the n-curves are now minima. Accordingly an interval of J values with non-hyperbolicity lies above the value of the saddle-centre bifurcation. In addition the arrangement of hyperbolic and inverse hyperbolic (elliptic) points is reflected. The exception here is the hyperbolic point corresponding to $n = 0$, which does not have an inverse hyperbolic or elliptic counter part. It has heteroclinic connections with the other unstable fixed points, as soon as they are created. Fully regular motion is reached again for $J < -0.457\,71\ldots$. Notice, though the bifurcation scenario is exactly the same as for $J > 0$ but in the inverse sense discussed above, the number of fixed points is always odd. Therefore the symbolic dynamic is constructed out of $N = 2n + 1$ symbols.

6. The two-disc scatterer

We now proceed to the system of two rotating discs with the same geometrical conditions (figure 1). The second disc is diametrically opposed to the first one with respect to the centre of rotation. This model is a billiard version of the Copenhagen problem in astronomy [8]. Our goal is to distinguish some pure three-body effects that arise in this case.

The relation between the Jacobi integral and α for the primitive periodic orbits that involve both discs is given by

$$J_{12}^{-} = \frac{\omega^2(R-d)^2}{2(n\pi-\alpha)^2}\left[\cos^2\alpha - (n\pi-\alpha)\sin 2\alpha\right] \tag{8}$$

$$J_{12}^{+} = \frac{\omega^2(R-d)^2}{2((n+1)\pi-\alpha)^2}\left[\cos^2\alpha - ((n+1)\pi-\alpha)\sin 2\alpha\right]. \tag{9}$$

Here, n has the same meaning as in (6), and J_{12}^{-}, J_{12}^{+} are the Jacobi integrals for a particle running against ($\alpha < 0$) or with ($\alpha > 0$) the rotation of the discs, respectively. In figure 12 we plot J_{12}^{-} and J_{12}^{+} as a function of the incoming angle for $n = 0, 1, 2$ and $\omega = 1.0$. Notice that for each n the curve J_{12}^{+} is joined smoothly to the corresponding $n+1$ of J_{12}^{-}.

All the periodic orbits for the one-disc model are found in the two-disc model, but this does not hold in the opposite sense. The periodic orbits formed by segments involving bounces with both discs are true three-body features. In figure 13 we plot for $J = 1$ the stable and unstable manifolds of a periodic orbit that hits both discs alternately ($\alpha \approx -1.270\ldots$). The iterates of these line segments come close to the other two fixed points building heteroclinic connections with their manifolds. The structure of the sections indicates the completeness of the horseshoe of three fixed points, implying a complete symbolic dynamics with three symbols. The scenario found for the one-disc scatterer is repeated here, with the addition of the two-disc orbits. Indeed the behaviour of the scattering functions described in section 3 for the two-disc model is qualitatively the same as for the one-disc case.

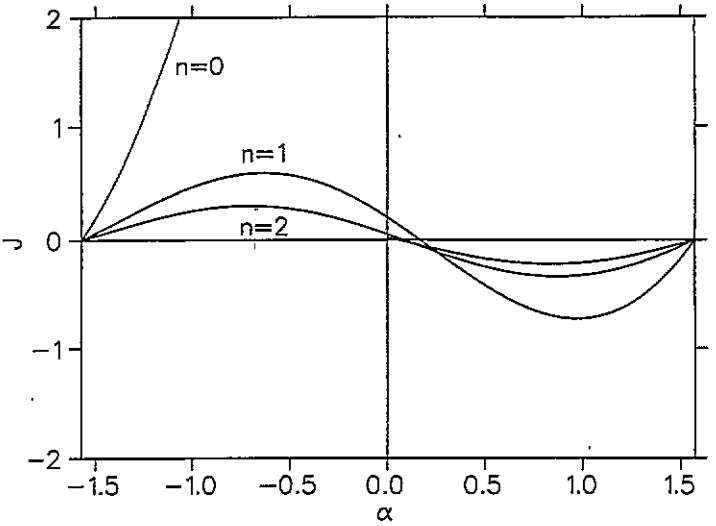

Figure 12. Behaviour of the Jacobi integral for the different primitive periodic orbits bouncing off both discs in the two-disc model as a function of the incidence angle α for radial collisions.

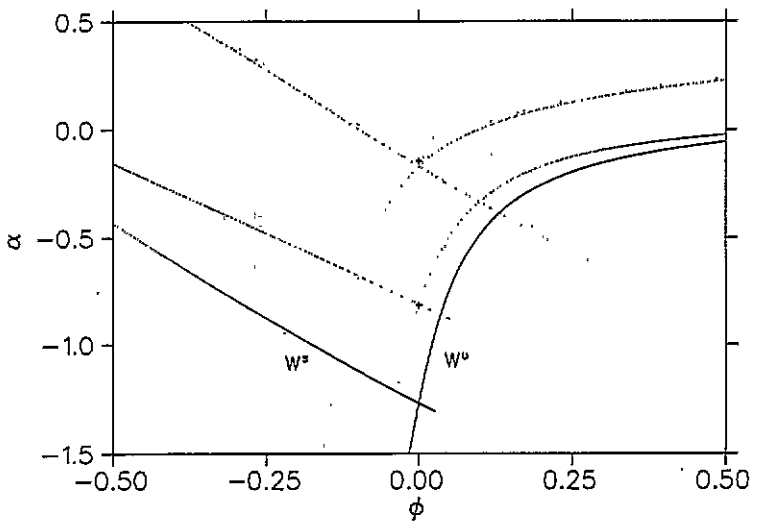

Figure 13. Stable and unstable manifolds for $J = 1.0$ of the fixed point belonging to the two-disc orbit. This plot is generated by iterates of the manifolds of only this fixed point. The other two fixed points are marked by crosses.

Note that the singularity in figure 12 for J_{12}^{-} for $n = 0$ at $\alpha = 0$ (when $\omega \neq 0$) comes from the infinite energy needed for the diametrical orbit to be completed without an increase in the number of turns n. The existence of this singularity implies that for any positive Jacobi integral there always exists one periodic orbit. Here the particle runs against the rotation of the discs and bounces off both alternately. This orbit is an example of a three-body effect and is also observed for the gravitational RTBP.

7. Conclusions

In the present paper we have studied the dynamics of scattering model systems which are inspired by the RTBP of astronomy and by scattering off a rotating diatomic molecule. We have found in both of our models that the system may display chaotic or regular behaviour depending on the value of the Jacobi integral. Furthermore, we have derived analytically all the primitive periodic orbits of the systems, which are the skeleton of the underlying dynamics. These orbits have the convenient property that they conserve the energy. When the value of the Jacobi integral is such that more than one primitive periodic orbit exists, homoclinic and heteroclinic intersections between their manifolds are observed, implying topological chaos giving rise to a fractal set of singularities in the scattering functions. This is due to the possibility of forming an infinite family of new periodic orbits being overshadowed by segments of the primitive ones allowed at the given value of the Jacobi integral. The grammar of those sequences depends on the Jacobi integral, since the homoclinic and heteroclinic intersections may or may not form a complete Smale horseshoe. For J approaching 0 the number of primitive periodic orbits in the invariant set grows without limit. For positive J this number is even, for negative J this number is odd. For any number of periodic orbits there is an interval of J-values in which the invariant set is completely hyperbolic. In this sense for the appropriate parameter interval our system contains completely hyperbolic horseshoes with any number of fixed points. The transition between regular and irregular behaviour is found to be a saddle-centre bifurcation.

It is interesting to note that the features responsible for the irregular behaviour in the one-disc model are repeated in the two-disc model with the addition of some new families of periodic orbits. These new families are constructed from the primitive orbits which bounce off both discs. We find qualitatively different behaviour for the $n = 0$ orbit which exists for all positive J. This will be the one feature we miss if we use a one-disc model to simulate properties of targets with two well defined centres.

In the case of $n = 0$, the primitive periodic orbits arising exclusively from J_{11} are two-body effects, since those orbits just involve one disc. In the two-disc case, the singularity of J_{12}^{-} at $\alpha = 0$ (which corresponds to the diametrical orbit that bounces both discs without letting the discs complete a turn over) is a true three-body effect, which does not influence the range of values on the Jacobi integral where irregular scattering is found. On the other hand, the curve J_{12}^{+} has an important effect on the behaviour of the system, since above its minimum homoclinic and heteroclinic intersections of the invariant manifolds are found, implying irregular behaviour of the system in a range of J where the one-disc model is regular.

Surprisingly, we found that both scattering billiard models possess stable periodic orbits and KAM tori for some small ranges of the Jacobi integral. This is quite pleasant since stable bounded orbits are also known in the gravitational RTBP.

The result of our classical models will also be interesting for comparison with corresponding quantum computations. In particular, it is known that there exists a close connection between classical periodic orbits and quantum behaviour. For the quantum treatment the possibility to transform to the rotating frame may be helpful since it avoids the time dependence. However, the quantum treatment in the rotating frame is only approximate because of the problems of quantization in a non-inertial frame.

Acknowledgments

The authors thank F J Elmer and W Breymann for useful discussions. This work was partially supported by the Swiss National Science Foundation and UNAM. CJ thanks the DFG for a Heisenberg stipendium.

References

[1] Lombardi M and Seligman T H 1993 *Phys. Rev.* A **47** 3571
[2] Delande D 1989 *Chaos and Quantum Physics (Les Houches Lectures Notes)* ed M J Giannoni *et al* (New York: North-Holland) 1992
[3] Smilansky U 1989 *Chaos and Quantum Physics (Les Houches Lectures Notes)* ed M J Giannoni *et al* (New York: North-Holland) 1992
[4] Brumer P and Shapiro M 1988 *Adv. Chem. Phys.* **70** 365
[5] Richter K and Wintgen D 1990 *J. Phys. B: At. Mol. Opt. Phys* **19** L197
[6] Boyd P T and McMillan S L 1992 *Phys. Rev.* A **46** 6277
[7] Whittaker E T 1989 *A Treatise on the Analytical Dynamics of Particles and Bodies* 4th edn (Cambridge: Cambridge University Press)
[8] Szebehely V 1967 *Theory of Orbits* (New York: Academic)
[9] Jung C and Scholz H J 1987 *J. Phys. A: Math. Gen.* **20** 3607
[10] Ding M, Grebogi C, Ott E and Yorke J A 1990 *Phys. Rev.* A **42** 7025
[11] Rückerl B and Jung C 1994 *J. Phys. A: Math. Gen.* **27** 55
[12] Troll G 1991 *Physica* **50D** 276
[13] Troll G 1992 *Nonlinearity* **5** 1151